

# Optimal Boundary Control of Convention-Reaction Transport Systems with Binary Control Functions

Falk M. Hante and Günter Leugering

Department Mathematik, Lehrstuhl für Angewandte Mathematik II, Universität  
Erlangen-Nürnberg, Martensstr. 3, 91058 Erlangen, Germany  
{hante,leugering}@am.uni-erlangen.de

**Abstract.** We investigate a new approach for solving boundary control problems for dynamical systems that are governed by transport equations, when the control function is restricted to binary values. We consider these problems as hybrid dynamical systems embedded with partial differential equations and present an optimality condition based on sensitivity analysis for the objective when the dynamics are governed by semilinear convection-reaction equations. These results make the hybrid problem accessible for continuous non-linear optimization techniques. For the computation of optimal solution approximations, we propose using meshfree solvers to overcome essential difficulties with numerical dissipation for these distributed hybrid systems. We compare results obtained by the proposed method with solutions taken from a mixed inter programming formulation of the control problem.

## 1 Introduction

Dynamical transport processes governed by first order hyperbolic *partial differential equations* (PDEs), in particular on metric graphs, model a wide variety of complex problems in civil engineering such as gas or traffic flow, but also many problems in chemical engineering as well as communication, information and logistic areas [14]. Often these problems involve decisions for controlling these dynamical processes at the boundaries, for instance turning on/off compressors, switching valves or toggle traffic lights [10].

We consider these multiscale problems as hybrid dynamical systems embedded with PDEs in which the implementation of switching is merely on a faster time scale than the transportation. With very few exceptions, noting [4,13,1,12], these problems have not been considered in the context of hybrid systems, though they represent a potentially rich field of study [3].

In context of PDE constraint optimization, mixed integer programming is used for solving such control problems, e. g. for gas network optimization [15,11], not least because of their obvious capability to consider the decision variables. The drawback of mixed integer models is certainly their computational complexity when the problems become large. Continuous non-linear optimization techniques

provide an alternative, though the treatment of discrete variables therein is not straightforward. Relaxation of the decision variables together with a penalty term homotopy provides a heuristic approach for solving such problems with non-linear optimization. It has for instance been applied for ramp metering of traffic flow [4], but in general this heuristic lacks convergence to the integer optimal solution [17]. We therefore investigate alternative methods for solving this hybrid control problem using continuous non-linear optimization that converge to (locally) optimal solutions.

Similar approaches are well-known for certain lumped parameter models that usually consist of switching among *ordinary differential equations* (ODEs) in a predefined sequence of active subsystems. Optimality conditions for piecewise defined solutions of ODEs were already developed in the 1960s in the context of ODE optimal control theory [7]. These optimality conditions were later considered for optimal control of hybrid dynamical systems governed by ODEs in [2,8].

The approach investigated here is based on a new optimality condition for switching boundary data when the system dynamics are governed by the semi-linear transport partial differential equation. For the computation of optimal switching signals we propose to use meshfree solvers in order to overcome essential difficulties with numerical dissipation when the distributed system is discretized in space using standard fixed Eulerian grids. To demonstrate the feasibility of our approach, we compare numerical results of our method with solutions obtained from a mixed integer programming formulation of this hybrid optimal control problem.

The paper is organized as follows. In Section 2, we give a detailed formulation of the problem we consider. In Section 3, we present a first order optimality condition based on sensitivity analysis. In Section 4, we sketch the main ideas of an appropriate numerical method to compute optimal solution approximations. In Section 5, we present numerical results for two model problems. In Section 6, we conclude with final remarks and directions for future work.

## 2 Problem Formulation

Consider material flow governed by the well-known convection-reaction transport equation

$$\frac{\partial}{\partial t}u(t, s) + \frac{\partial}{\partial s}[a(t, s)u(t, s)] = f(t, s, u(t, s)), \quad s \in [0, 1], \quad t > 0 \quad (1)$$

for the unknown scalar function  $u(t, s)$ . Assuming that  $a > 0$ , the material inflow at  $s = 0$  shall be given by boundary data

$$u(t, 0) = \hat{u}(t; \mu(t)), \quad t \geq 0, \quad (2)$$

where the inflow  $\hat{u}$  is controlled by a parameter  $\mu(t)$ . The material distribution at  $t = 0$  shall be given by initial data

$$u(0, s) = \bar{u}(s), \quad 0 < s < 1. \quad (3)$$

We introduce hybridness into the problem in that the control  $\mu(\cdot)$  of the material inflow  $\hat{u}$  is a decision variable taking values in a discrete set. We will here assume for simplicity  $\mu(t) \in \{0, 1\}$ ,  $t \geq 0$ . An admissible control is a switching signal  $\mu(\cdot)$  which has only finitely many switches  $\mu \curvearrowright \mu'$  ( $\mu \neq \mu' \in \{0, 1\}$ ) with corresponding switching time  $\tau_k$  in each finite time interval.

Embedding (1)–(3) into a graph setting, these equations model a variety of realistic network flow problems. For a given graph  $(E, N)$  with edges  $e_i \in E$  and nodes  $n_j \in N$ , one can identify each edge with an interval  $[0, 1]$  and consider a PDE (1) along each of those edges. At multiple nodes  $n_j$  the boundary condition (2) is then to be replaced by a nodal condition, e.g. the sum of all in- and outflows equals a given nodal control  $\hat{u}(t; \mu(t))$ . See, e.g. [18] for details on such a network flow model applied to air traffic flow.

As performance index of the system over a finite time horizon  $[0, T]$ , we consider the integral of any continuous functional  $g(\cdot)[\cdot, \cdot]$ , e.g.

$$\int_0^T \int_0^1 g(u)[t, s] ds dt = \int_0^T \int_0^1 |u(t, s) - u_d(t, s)|^2 ds dt, \tag{4}$$

measuring the  $L^2$ -distance of the solution  $u$  to a desired solution  $u_d$ , together with costs  $\gamma(\tau_k)$  for switching  $\mu \curvearrowright \mu'$  at  $\tau_k$ . As the optimal boundary control of the system (1)–(3) with continuous variables is well-understood, we consider here the discrete control  $\mu$  as the only control variable. Thus the control task is to minimize

$$J = \int_0^T \int_0^1 g(u)[t, s] ds dt + \sum_{\tau_k} \gamma(\tau_k). \tag{5}$$

by specifying the switching function  $\mu(\cdot)$  on  $[0, T]$ , where  $u(\cdot, \cdot)$  solves the continuous transport equation (1)–(3).

It is easy to see that (1) together with possibly discontinuous boundary data (2) does not possess a classical, continuously differentiable solution. As common for conservation laws, we will therefore consider solutions in a broad sense having bounded variation as given by the method of characteristics. For any point  $(\tau, \sigma) \in \Omega := \{(t, s) : t \geq 0, 0 \leq s \leq 1\}$ , we denote by  $t \mapsto s(t; \tau, \sigma)$  the characteristic curve passing through  $(\tau, \sigma)$ , i.e. the solution of the ODE initial value problem

$$\frac{d}{dt} s(t) = a(t, s(t)), \quad s(\tau) = \sigma. \tag{6}$$

If  $s(t)$  solves (6) at any time  $t$ , one has

$$\frac{d}{dt} u(t, s(t)) = \frac{\partial}{\partial t} u + \frac{d}{dt} s(t) \frac{\partial}{\partial s} u = \frac{\partial}{\partial t} u + a(t, s) \frac{\partial}{\partial s} u = \tilde{f}(t, s(t), u), \tag{7}$$

where

$$\tilde{f}(t, s, u) = f(t, s, u) - \frac{\partial}{\partial s} a(t, s). \tag{8}$$

The value of the *broad solution*  $u$  of (1)–(3) at any point  $(\tau, \sigma) \in \Omega$  is then defined [5] as the value at time  $\tau$  of the ODE initial value problem

$$\frac{d}{dt} u = \tilde{f}(t, s(t; \tau, \sigma), u), \quad u(t^*) = data \tag{9}$$

where  $t^*$  denotes the time when the curve  $s(\cdot; \tau, \sigma)$  intersects the boundary of  $\Omega$  and  $data$  is the prescribed initial/boundary data there.

We consider this hybrid control problem under the following hypotheses:

- (H<sub>1</sub>) The initial data  $\bar{u}(\cdot)$  and, for all modes  $\mu$  fixed, the boundary data  $\hat{u}(\cdot; \mu)$  is continuous.
- (H<sub>2</sub>) The convection term  $a(\cdot, \cdot)$  is continuous in  $t$  and twice continuously differentiable in  $s$ , positive, bounded and bounded away from 0. Moreover,  $a(\cdot, \cdot)$  satisfies a bound of the form  $|a(t, s)| \leq C_1(1 + |s|)$  uniformly in  $t$ .
- (H<sub>3</sub>) The reaction term  $f(\cdot, \cdot, \cdot)$  is continuous in  $t, s$  and is Lipschitz continuous in  $u$ . Additionally,  $f(\cdot, \cdot, \cdot)$  satisfies a bound of the form  $|f(t, s, u)| \leq C_2(1 + |u|)$  uniformly in  $t$  and  $s$ .
- (H<sub>4</sub>) The functional  $g(\cdot)$  is continuous in  $u$ .
- (H<sub>5</sub>) The switching cost  $\gamma(\cdot)$  is continuously differentiable, positive and bounded below by a constant  $\underline{\gamma}$ .
- (H<sub>6</sub>) For some reference control  $\bar{\mu}$ , the cost  $J$  is finite.

For details on wellposedness of the problem, in particular in the case of a network setting, we refer to [12]. We just note that standard results in the theory of ODEs imply that the solutions (in the sense of Carathéodory) of (6) and (9) exist, are bounded for bounded initial/boundary data and depend on the point  $(\tau, \sigma)$  in a continuously differentiable way. Moreover, hypothesis (H<sub>5</sub>) and (H<sub>6</sub>) bound the number of switches for the optimal control by

$$K = \left\lceil \frac{J(\bar{\mu})}{\underline{\gamma}} \right\rceil. \tag{10}$$

Latter can be easily seen by assuming that there exists an optimal control  $\mu^*$  with more than  $K$  switches. The optimal value then satisfies  $J(\mu^*) > K\underline{\gamma}$  because  $\underline{\gamma}$  is a lower bound of the positive switching cost. On the other hand, from the bound (10) we have  $J(\bar{\mu}) = K\underline{\gamma}$ , contradicting the optimality of  $\mu^*$ . A compactness argument then yields the following result.

**Theorem 1 ([12]).** *There exists an optimal switching signal  $\mu^*$  minimizing (5) subject to (1), (2) and (3). □*

Our goal is to use gradient based optimization methods to compute (locally) optimal  $\mu^*$ . The key idea is to fix  $\mu(0)$  by  $\mu_0 \in \{0, 1\}$  and thus all subsequent modes and, using the bound  $K$  given in (10), to obtain  $\mu^*$  by considering  $\tau_k$  as the new (continuous) optimization variables subject to appropriate inequality constraints, i. e.  $\mu^*$  is obtained solving

$$\begin{aligned} & \min_{0 \leq \tau_1 \leq \dots \leq \tau_K \leq T} J[u, \tau_1, \dots, \tau_K] \\ & \text{s. t. } u \text{ solves (1), (2), (3).} \end{aligned} \tag{11}$$

Note that in problem (11) the continuous control  $\hat{u}(t, \mu_k)$  for fixed  $\mu_k$  on the interswitching intervals  $[\tau_k, \tau_{k+1}]$  is not subject to optimization, but the switching times  $\tau_k$  are. We present a first order optimality condition for this problem in the next section, noting that this is an essential subproblem of the two stage problem involving in addition the optimization of  $\hat{u}(t, \mu_k)$ .

### 3 Optimality Condition

The optimality condition for optimal  $\tau_k$  in (11) is mainly based on the following sensitivity result.

**Theorem 2.** *Consider the problem (11) under the hypotheses (H<sub>1</sub>)–(H<sub>6</sub>) and let  $0 < \tau_1 < \dots < \tau_K < T$ . Then, for all  $k = 1, \dots, K$ ,*

$$\frac{\partial}{\partial \tau_k} J = \int_{\tau_k}^{t^*(\tau_k)} (g(u^{\tau_k+})[t, s^*(t, \tau_k)] - g(u^{\tau_k-})[t, s^*(t, \tau_k)]) \frac{\partial}{\partial \tau_k} s^*(t, \tau_k) dt + \frac{d}{d\tau_k} \gamma(\tau_k),$$

where  $s^*(\cdot, \tau_k)$  solves the characteristic equation (6) with  $\tau = \tau_k$  and  $\sigma = 0$ ,  $t^*(\tau_k) = \max\{t \in [0, T] : s^*(t, \tau_k) \leq 1\}$  and where  $u^{\tau_k+}$ ,  $u^{\tau_k-}$  denote the solutions of (1), (2), (3) with  $u(\tau_k, 0) = \hat{u}(\tau_k; \mu(\tau_{k+1}))$ ,  $u(\tau_k, 0) = \hat{u}(\tau_k; \mu(\tau_k-))$ , respectively.

*Proof.* Fix  $k \in \{1, \dots, K\}$  and let  $\tau_1, \dots, \tau_K$ ,  $s^*(\cdot, \tau_k)$  and  $t^*(\tau_k)$  be given as stated in Theorem 2. The cost function can be split up as follows

$$J = \sum_{k=1}^K \gamma(\tau_k) + \int_0^{\tau_k} \int_0^1 g(u^{\tau_k-})[t, s] ds dt + \int_{t^*(\tau_k)}^T \int_0^1 g(u^{\tau_k+})[t, s] ds dt + \\ + \int_{\tau_k}^{t^*(\tau_k)} \int_0^{s^*(t, \tau_k)} g(u^{\tau_k+})[t, s] ds dt + \int_{\tau_k}^{t^*(\tau_k)} \int_{s^*(t, \tau_k)}^1 g(u^{\tau_k-})[t, s] ds dt.$$

Thus, under hypotheses (H<sub>1</sub>)–(H<sub>6</sub>), we have

$$\frac{\partial}{\partial \tau_k} J = \frac{d}{d\tau_k} \gamma(\tau_k) + \int_0^1 g(u^{\tau_k-})[\tau_k, s] ds - \int_0^1 g(u^{\tau_k+})[t^*(\tau_k), s] ds \frac{\partial}{\partial \tau_k} t^*(\tau_k) + \\ + \int_{\tau_k}^{t^*(\tau_k)} g(u^{\tau_k+})[t, s^*(t, \tau_k)] \frac{\partial}{\partial \tau_k} s^*(t, \tau_k) dt + \\ - \int_0^{s^*(\tau_k, \tau_k)} g(u^{\tau_k+})[\tau_k, s] ds + \int_0^{s^*(t^*(\tau_k), \tau_k)} g(u^{\tau_k+})[t^*(\tau_k), s] ds \frac{\partial}{\partial \tau_k} t^*(\tau_k) + \\ - \int_{\tau_k}^{t^*(\tau_k)} g(u^{\tau_k-})[t, s^*(t, \tau_k)] \frac{\partial}{\partial \tau_k} s^*(t, \tau_k) dt + \\ - \int_{s^*(\tau_k, \tau_k)}^1 g(u^{\tau_k-})[\tau_k, s] ds + \int_{s^*(t^*(\tau_k), \tau_k)}^1 g(u^{\tau_k-})[t^*(\tau_k), s] ds \frac{\partial}{\partial \tau_k} t^*(\tau_k) \\ = \int_{\tau_k}^{t^*(\tau_k)} (g(u^{\tau_k+})[t, s^*(t, \tau_k)] - g(u^{\tau_k-})[t, s^*(t, \tau_k)]) \frac{\partial}{\partial \tau_k} s^*(t, \tau_k) dt + \frac{d}{d\tau_k} \gamma(\tau_k),$$

where the sum of all integrals in  $s$  vanish, using that  $s^*(\tau_k, \tau_k) = 0$  and that  $s^*(t^*(\tau_k), \tau_k) = 1$ . □

*Remark 1.* From the equation for  $\frac{\partial}{\partial \tau_k} J$  in Theorem 2, it is easy to see that the mapping  $\tau \mapsto \sum_{k=1}^K \frac{\partial}{\partial \tau_k} J$  is continuous for all switching times  $\tau_k$  satisfying  $0 < \tau_1 < \dots < \tau_K < T$  using (H<sub>4</sub>) and that  $\tau_k \mapsto \frac{\partial}{\partial \tau_k} s^*(t, \tau_k)$  is continuous due to (H<sub>2</sub>). But in the case that  $\tau_k = \tau_{k+1}$  for some  $k$ , the derivative  $\frac{\partial}{\partial \tau_k} J$  is not defined. However, the mapping  $\tau_k \mapsto \frac{\partial}{\partial \tau_k} J$  can be continued in such points continuously by restricting the domain of  $g(u^{\tau_k^-})[t, s^*(t, \cdot)]$  to the single point  $\tau_k = \tau_{k+1}$ .

Based on Theorem 2 and Remark 1 the Karush-Kuhn-Tucker first order necessary optimality conditions taking into account the special structure of the constraints  $0 \leq \tau_1 \leq \dots \leq \tau_K \leq T$  can be stated as follows.

**Proposition 1.** *Let  $\tau^* = (\tau_1^*, \dots, \tau_K^*)$  be a local minimum of (11) under the hypotheses (H<sub>1</sub>)–(H<sub>6</sub>). Then, for all  $k = 1, \dots, K$ ,*

$$\sum_{i=\kappa(k)}^k \frac{\partial J(\tau^*)}{\partial \tau_i^*} \leq 0 \text{ unless } \tau_k^* = 0, \quad \text{and} \quad \sum_{i=k}^{\eta(k)} \frac{\partial J(\tau^*)}{\partial \tau_i^*} \geq 0 \text{ unless } \tau_k^* = T, \quad (12)$$

where  $\kappa(k) = \min\{0 \leq \kappa \leq k : \tau_\kappa^* = \tau_k^*\}$ ,  $\eta(k) = \max\{K + 1 \geq \eta \geq k : \tau_\eta^* = \tau_k^*\}$  with  $\tau_0^* := 0$  and  $\tau_{K+1}^* := T$ .

*Proof.* See [8]. □

### 4 Computational Remarks

A major difficulty of this problem comes with the fact that, in order to evaluate the cost function  $J$ , one needs to discretize and solve the PDE constraint in space and time. In order to apply non-linear optimization techniques, it is necessary to ensure that the discretized solution  $\tilde{u}(\cdot, \cdot)$  depends continuously on the optimization variables  $\tau_1, \dots, \tau_K$ . Careless re-meshing in every step of the optimizer may easily destroy this property. For the problem (11) continuous dependence of the mapping  $(\tau_1, \dots, \tau_K) \mapsto \tilde{u}(\cdot, \cdot)$  can be achieved by using adaptive time steps  $\Delta t$ . However, for time steps  $\Delta t$  much smaller than the discretization step size  $h$  of any fixed Eulerian grid in space, the numerical dissipation, e. g.

$$\frac{1}{2}(a(t, s)\Delta t - h)a(t, s)\frac{\partial^2}{\partial s^2}u(t, s) \tag{13}$$

for upwind finite differencing discretization schemes, becomes large and causes inaccurate solution approximations.

We overcome this difficulty by using meshfree numerical solvers for such a hybrid transport problem. Points representing the solution are moved according to their characteristic velocity. These schemes are capable of propagating

discontinuities in the solution with correct speed and they are free of numerical dissipation. In case of a semilinear equation (1), the method is easy to implement but rarely used. We will briefly sketch the method here, noting that similar particle management for the case of non-linear conservation laws has been proposed recently [9].

*Sketch of the meshfree solver*

1. The initial solution is the approximation of the initial data (3) by a finite number of points  $s_1 < \dots < s_m \in (0, 1)$  with function values  $u_1, \dots, u_m$  for some  $m \in \mathbb{N}$ .
2. The solution over time is found by
  - (a) Moving each point  $s_i$  with speed  $a(t, s)$  as suggested by (6).
  - (b) Updating the function values  $u_i$  by solving an integral formulation of  $\dot{u} = f(t, s, u)$ , compare (7).
  - (c) Inserting points where the distance between two points or their distance to  $s = 0$  becomes unsatisfyingly large. When points are inserted at  $s = 0$ , their function value is taken from an approximation of the boundary data (2).
  - (d) Dropping all points that are no longer needed, i. e. those with  $s_i > 1$ . □

Many efficient adaptive sampling strategies for the initial and boundary data can be used because there is no requirement on the point distribution  $s_i$ . In particular, one may approximate the boundary data  $\hat{u}$  at the switching times  $\tau_k$  and at a fixed number of equidistant time instances during interswitching intervals  $[\tau_k, \tau_{k+1}]$ . This strategy ensures that the discretized solution depends continuously on the switching times as desired. The method is as accurate as the movement of  $s_i$  and the updates of  $u_i$  are realized. In particular, using explicit Euler methods makes the piecewise constant solution approximation  $\tilde{u}(\cdot, \cdot)$  first order accurate everywhere and the solver in pseudo-code reads as follows.

**Algorithm 1 (Meshfree solver)**

```

Require:  $a, \tilde{f}, \bar{u}, \tilde{u}, \tau_1, \dots, \tau_K$ .
Initialize:  $\tau_0 := 0, \tau_{K+1} := 1, \Delta h := \frac{1}{m}$ 
            $[s] := [s_1, \dots, s_m]$  with  $s_i = i * \Delta h$ 
            $[u] := [u_1, \dots, u_m]$  with  $u_i = \bar{u}(s_i)$ 
for  $k = 0, \dots, K + 1$  do
     $\Delta t := (\tau_{k+1} - \tau_k) / N$ 
    for  $j = 1, \dots, N$  do
         $t := \tau_k + j * \Delta t$ 
        Memorize:  $\tilde{u}(t, [s]) := [u]$ 
        Move:  $[s] := [s] + \Delta t * a(t, [s])$ 
        Update:  $[u] := [u] + \Delta t * \tilde{f}(t, [s], [u])$ 
    for all  $i$  such that  $s_{i+1} - s_i > \Delta h$  do
        Insert:  $[s] := [[s]_{\leq i}, \frac{s_i + s_{i+1}}{2}, [s]_{\geq i+1}], [u] := [[u]_{\leq i}, \frac{u_i + u_{i+1}}{2}, [u]_{\geq i+1}]$ 
    end for

```

**if**  $s_1 > \Delta h$  **then**

*Insert:*  $[s] := [0, [s]], [u] := [\hat{u}(t; \mu(t)), [u]]$

**end if**

*Drop:*  $[s] := [s]_{I \setminus J}$  with  $I = \{1, \dots, \text{length}([s])\}$ ,  $J = \{i \in I : s_i > 1\}$

**end for**

**end for**

With the solution approximation  $\tilde{u}(\cdot, \cdot)$  obtained from the meshfree solver not all information is readily available to evaluate  $\frac{\partial}{\partial \tau_k} J$  as given in Theorem 2 for applying a gradient based optimization method solving the optimality system given in Proposition 1. Additionally, the solutions of  $s^*(t, \tau_k)$  and  $\frac{\partial}{\partial \tau_k} s^*(t, \tau_k)$  are needed. While the former can be directly computed using (6), the latter can be obtained using the following Lemma.

**Lemma 1.** *Let  $s^*(t, \tau_k)$  solve the characteristic equation (6) with  $\tau = \tau_k$  and  $\sigma = 0$ . Then,  $\frac{\partial}{\partial \tau_k} s^*(t, \tau_k) = \Phi(t, \tau_k)$ , where  $\Phi(\theta, \tau_k)$  is the state transition matrix of the following linear time varying dynamical system*

$$\frac{d}{d\theta} z(\theta) = \frac{\partial}{\partial s} a(\theta, s) \Big|_{s=s^*(\theta, \tau_k)} z(\theta) \tag{14}$$

*Proof.* Let  $z(\theta) = \frac{\partial}{\partial \tau_k} s^*(\theta, \tau_k)$ . Then, the statement of the Lemma follows from the derivation

$$\begin{aligned} \frac{d}{d\theta} z(\theta) &= \frac{d}{d\theta} \frac{\partial}{\partial \tau_k} s^*(\theta, \tau_k) = \frac{\partial}{\partial \tau_k} \frac{d}{d\theta} s^*(\theta, \tau_k) = \frac{\partial}{\partial \tau_k} a(\theta, s^*(\theta, \tau_k)) \\ &= \frac{\partial}{\partial s} a(\theta, s) \Big|_{s=s^*(\theta, \tau_k)} \frac{\partial}{\partial \tau_k} s^*(\theta, \tau_k) = \frac{\partial}{\partial s} a(\theta, s) \Big|_{s=s^*(\theta, \tau_k)} z(\theta). \quad \square \end{aligned}$$

In the following section, we compare numerical results for a gradient based optimization method established on the results presented in this section.

## 5 Numerical Results

We present numerical results for two model problems. For both we compare the following two methods to compute approximations of (locally) optimal binary control functions  $\mu^*(\cdot)$  that minimize (5).

*COPT.* This methods applies continuous non-linear optimization techniques for the reformulated problem (11) using the results presented in Section 3 and Section 4. The system (1) is solved using a meshfree solver, which realizes the movement of  $s_i$  and the updates of  $u_i$  in our implementation by explicit Euler methods, see Algorithm 1. The cost function is approximated by the trapezoidal rule. The search for locally optimal  $\tau_k$  (specifying  $\mu(\cdot)$ ) is carried out by the MATLAB sequential quadratic programming solver *fmincon* [19]. The gradients for the BFGS updates are computed using the formula given in Theorem 2. Termination criterion is the first order optimality measure or the norm of the directional derivative falling below tolerance.



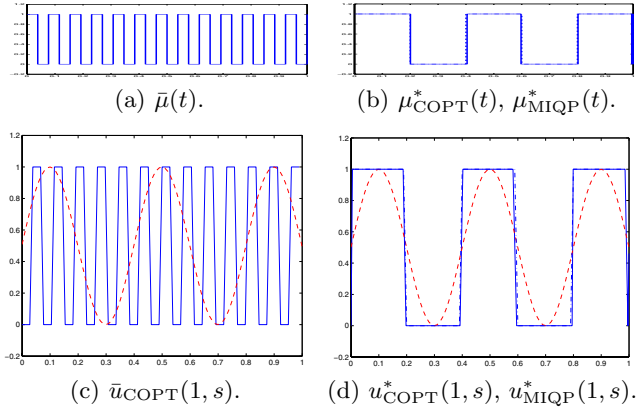


**Fig. 1.** Initial and optimal bang-bang type solution of the traveling sine wave in Example 1. Fig. (a) and (c) show the initial switching signal with a final time plot of the corresponding solution. Fig. (b) and (d) show the computed optimal switching signals with corresponding solutions at  $t = T = 1$  (COPT solutions solid, MIQP solutions dash-dotted). The dashed curve in Fig. (c) and (d) show the desired wave  $u_d$  plotted at final time  $T = 1$ .

*MIQP.* This method uses mixed integer programming on the original problem. The system dynamics (1) are transformed into a linear system constructed by upwind finite difference discretization on a fixed, equidistant Eulerian grid. For each timestep  $t_k$ , a binary variable represents  $\mu(t_k)$ . The cost function is approximated by the trapezoidal rule. We included the details on the MIQP reformulation in Appendix A, noting that more sophisticated MIQP reformulations of this problem are possible. The reformulation chosen here shall primarily serve as a verification of the proposed method above. The search for the obtained equality constraint mixed integer quadratic program is carried out by ILOG CPLEX [6]. The solver terminates when the gap between the best integer objective and the objective of the best node remaining in the branch-and-bound tree falls below tolerance.

The first very simple example serves as a verification of the proposed method COPT for computing approximations of optimal switching control functions.

*Example 1.* (Bang-bang type approximation of a traveling sine wave.) The control task consists of approximating a traveling sine wave  $u_d$  by switching  $\hat{u}$  between the two extremal values of the wave  $\hat{u}_1 = 0$ ,  $\hat{u}_2 = 1$ . We assume that the wave speed equals the transportation velocity, here taken for simplicity as  $a(t, s) = 1$ . We also assume constant switching costs  $\gamma(\cdot) = 0.0075$  to avoid chattering. It should be clear that for this problem, we cannot expect exact controllability, but we are seeking for a binary control  $\mu^*(\cdot)$  minimizing the  $L^2$ -distance (4) between  $u$  and  $u_d$  over the finite time horizon  $[0, T]$  with  $T = 1$ . Also observe that the optimal control of the relaxed problem with  $\hat{u} \in [0, 1]$  is not

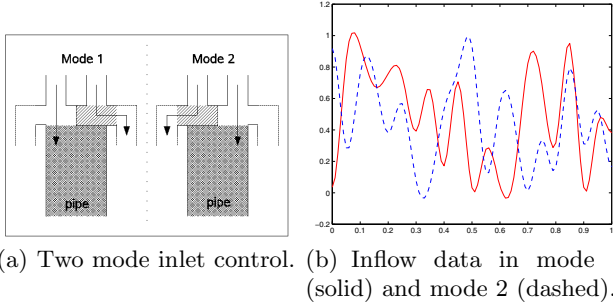


**Fig. 2.** Control task in Example 2

of bang-bang type. Thus, alternative methods like COPT or MIQP are required for the computation of optimal controls. For initialization of the continuous optimizer, we use  $\bar{\mu}(\cdot)$  given by  $\bar{\tau}_1, \dots, \bar{\tau}_K$  with  $K = 25$  equidistantly placed in  $[0, T]$  as depicted in Figure 1 (a). The cost of the initial solution that is shown in Figure 1 (c) is  $J(\bar{\mu}) = 0.1869$ .

COPT terminates after 11 iterations with an optimal value of  $J(\mu_{\text{COPT}}^*) = 0.0299$  and first order optimality measure of 0.0092, where 20 of the 25 initial switching times coalesce in the optimal solution approximation. The integer optimal solution  $\mu_{\text{MIQP}}^*$  for the upwind-discretized problem obtained by MIQP on a fixed grid with 2500 discretization points is qualitatively the same with  $J(\mu_{\text{MIQP}}^*) = 0.0298$ .

Plots of  $\mu_{\text{COPT}}^*$  (solid line) and  $\mu_{\text{MIQP}}^*$  (dashed line) are shown in Figure 1 (b) while the corresponding final time plots of the solution  $u$  at  $t = T = 1$  are shown in Figure 1 (d). Note that the example is chosen such that at time  $T$  the complete history of the boundary control action  $\mu(\cdot)$  is visible in  $u(T, s)$ .

The second example demonstrates that the method COPT may even outperform our mixed integer optimal programming implementation due to its inferiority in the discretization of the dynamical system.

*Example 2.* (2-mode plug flow regulation.) Consider a pipe that can be controlled at the inlet by choosing the inflow of material concentration either from  $\hat{u}_1$  or from  $\hat{u}_2$ , compare Figure 2 (a). The plug flow in the pipe is assumed to satisfy the conservation law

$$\frac{\partial}{\partial t} u(t, s) + \frac{\partial}{\partial s} [a(s)u(t, s)] = 0 \tag{15}$$

with  $a(s) = \frac{4}{3}(s - 1)^2 + \frac{1}{2}$ . The desired material distribution in the pipe is given by  $u_d(t, s) = \frac{1}{2}(s + 1)^2$ . As in Example 1, we cannot expect exact controllability, but we are again seeking for a binary control  $\mu^*(\cdot)$  minimizing the  $L^2$ -distance (4) between  $u$  and  $u_d$  over the finite time horizon  $[0, 1]$  and include switching costs  $\gamma(\cdot) = 0.0075$  to avoid chattering. For initialization of the continuous optimizer, we use  $\bar{\mu}(\cdot)$  with 35 equidistantly placed switching times  $\tau_k$  with a corresponding cost of  $J(\bar{\mu}) = 0.1693$ .

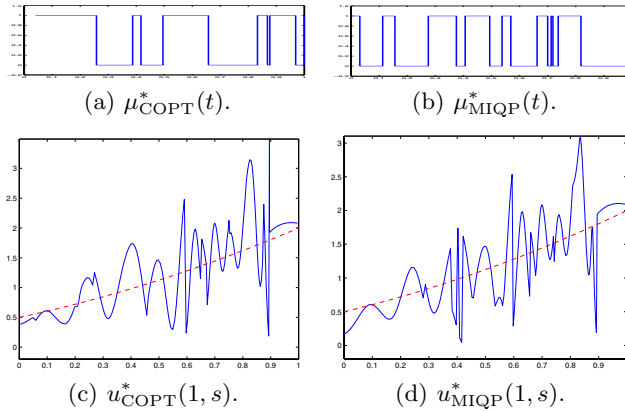


**Fig. 3.** Optimal control approximations for Example 2. Fig. (a) and (c) show the optimal switching signal computed with COPT and the final time plot of the corresponding solution  $u$  with  $J(\mu_{\text{COPT}}^*) = 0.0914$ . Fig. (b) and (d) show the MIQP result with  $J(\mu_{\text{MIQP}}^*) = 0.2694$ . The dashed line in Fig. (c) and (d) is the desired material distribution  $u_d$ .

COPT terminates after 17 iterations with an optimal value of  $J(\mu_{\text{COPT}}^*) = 0.0914$  and first order optimality measure of 0.01. The integer optimal solution  $\mu_{\text{MIQP}}^*$  for the upwind-discretized problem obtained by MIQP on a fixed grid with 12800 discretization points has an optimal value of  $J(\mu_{\text{MIQP}}^*) = 0.2694$ . The optimal control approximations  $\mu_{\text{COPT}}^*$  and  $\mu_{\text{MIQP}}^*$  with corresponding final time plots of the solutions at  $t = T = 1$  are depicted in Figure 3.

We finally remark that the choice of the initial condition  $\bar{\mu}(\cdot)$  is crucial for the proposed method since it searches for locally optimal controls only. A direct comparison with mixed integer programming, searching for globally optimal solutions on the discretized problem but at exponential cost, therefore is not feasible.

## 6 Conclusion

We presented a new approach for solving optimal boundary control problems for dynamical systems that are governed by semilinear transport equations when the control function is restricted to binary values. By considering this problem as a hybrid dynamical system embedded with partial differential equations, we derived an optimality condition similar to results known for hybrid systems governed by ordinary differential equations. This result makes the problem accessible for gradient based non-linear optimization methods.

For the computation of optimal solution approximations, we used meshfree solvers to overcome essential difficulties with numerical dissipation for these distributed hybrid systems. Our numerical results for model problems show that the proposed approach is a promising alternative compared to mixed integer programming.

Future work will be devoted to extend this approach to control problems that are governed by non-linear transport equations and multi-dimensional systems of equations.

## Acknowledgments

This work has been supported by the Elite Network of Bavaria within the project #K-NW-2004-143.

## References

1. Amin, S., Hante, F.M., Bayen, A.M.: On stability of switched linear hyperbolic conservation laws with reflecting boundaries. In: Egerstedt, M., Mishra, B. (eds.) HSCC 2008. LNCS, vol. 4981, pp. 602–605. Springer, Heidelberg (2008)
2. Xu, X., Antsaklis, P.: Optimal control of switched autonomous systems. In: Proc. IEEE Conf. Decision and Control, Las Vegas, NV (December 2002)
3. Barton, P.I.: Modeling, Simulation and Sensitivity Analysis of Hybrid Systems. In: Proc. of the IEEE Int. Symposium on Computer-Aided Control System Design, Anchorage, Alaska, September 25–27 (2000)
4. Bayen, A.M., Raffard, R.L., Tomlin, C.J.: Network congestion alleviation using adjoint hybrid control: Application to highways. In: Alur, R., Pappas, G.J. (eds.) HSCC 2004. LNCS, vol. 2993, pp. 95–110. Springer, Heidelberg (2004)
5. Bressan, A.: Hyperbolic Systems of Conservation Laws. Oxford University Press, New York (2000)
6. ILOG, Inc.: ILOG CPLEX Version 9.1, Sunnyvale, CA, USA (2007)
7. Dyer, P., McReynolds, S.R.: The Computation and Theorie of Optimal Control. Series Mathematics in Science and Engineering, vol. 65. Academic Press, New York (1970)
8. Egerstedt, M., Wardi, Y., Axelsson, H.: Transition-Time Optimization for Switched-Mode Dynamical Systems. IEEE Transactions on Automatic Control 51(1), 110–115 (2006)
9. Farjoun, Y., Seibold, B.: Solving One Dimensional Scalar Conservation Laws by Particle Management (January 2008) arXiv:0801.1495 [math.NA]
10. Fügenschuh, A., Herty, M., Klar, A., Martin, A.: Combinatorial and Continuous Models for the Optimization of Traffic Flows on Networks. SIAM Journal on Optimization 16, 1155–1176 (2006)
11. Geißler, B., Kolb, O., Lang, J., Leugering, G., Martin, A., Morsi, A.: Mixed Integer Linear Models for the Optimization of Dynamical Transport Networks (submitted, 2008)
12. Hante, F.M., Leugering, G., Seidman, T.I.: Modeling and Analysis of Modal Switching in Networked Transport Systems. Applied Mathematics and Optimization (in print) (2008) DOI:10.1007/s00245-008-9057-6
13. Kleinert, T., Lunze, J.: Modelling and state observation of Simulated Moving Bed processes based on an explicit functional wave form description. Mathematics and Computers in Simulation 68(3), 235–270 (2005)
14. Leugering, G.: Optimization and control of transport processes on networked systems. In: Conf. on Control of Physical Systems and Partial Differential Equations, Paris, June 16–20 (2008)

15. Martin, A., Möller, M., Moritz, S.: Mixed Integer Models for the Stationary Case of Gas Network Optimization. *Math. Program., Ser. B* 105, 563–582 (2006)
16. Quarteroni, A., Valli, A.: Numerical Approximation of Partial Differential Equations. 2. corr. printing. Springer, Berlin (1997)
17. Sager, S., Bock, H.G., Diehl, M., Reinelt, G., Schlöder, J.P.: Numerical Methods for Optimal Control with Binary Control Functions Applied to a Lotka-Volterra Type Fishing Problem. In: Seeger, A. (ed.) *Recent Advances in Optimization*. LNEMS, vol. 563, pp. 269–289. Springer, Heidelberg (2006)
18. Sun, D., Strub, I., Bayen, M.: Comparison of the performance of four Eulerian network flow models for strategic air traffic flow management. *Networks and Heterogeneous Media* 2(4), 569–594 (2007)
19. The Mathworks, Inc.: Matlab Release 7.5.0 (R2007b), Natick, MA, USA (2007)

## A Appendix: MIQP Formulation

For the sake of completeness we add the mixed integer formulation of the control problem (5) that was used for comparison in Example 1 and Example 2. In order to discretize a mixed initial boundary value problem of the type

$$\begin{aligned} \frac{\partial}{\partial t}u(t, s) + a(t, s) \frac{\partial}{\partial s}u(t, s) &= f(t, s) u(t, s) \quad s \in [0, 1], t > 0 \\ u(t, 0) &= \hat{u}(t; \mu(t)), \quad t \geq 0 \\ u(0, s) &= \bar{u}(s), \quad s \in (0, 1) \end{aligned} \quad (16)$$

we use an explicit upwind finite difference scheme (see e.g. [16], Sec. 14.2), coupled with integer programming. The space-time domain is discretized by choosing a time step  $\Delta t = 1/N$  and a mesh-width  $\Delta s = 1/M$ . The grid-points  $(t_j, s_i)$  are defined by

$$t_j = (j - 1)\Delta t, \quad j = 1, \dots, N, \quad s_i = (i - 1)\Delta s, \quad i = 1, \dots, M. \quad (17)$$

We replace the derivatives in the system (16) by upwind finite differences (using that  $a(\cdot, \cdot) > 0$ )

$$\frac{U_i(t_{j+1}) - U_i(t_j)}{\Delta t} + a(t_j, s_i) \frac{U_i(t_j) - U_{i-1}(t_j)}{\Delta s} = f(t_j, s_i) U_i(t_j) \quad (18)$$

for  $i = 2, \dots, M$  and  $j = 2, \dots, N$  and the initial condition becomes

$$U_i(t_1) = \bar{u}(s_i), \quad i = 2, \dots, M. \quad (19)$$

On the time grid the discrete control  $\mu(\cdot)$  can be represented by  $N$  binary values  $\mu_j \in \{0, 1\}$  and thus the boundary conditions can be written as

$$U_1(t_j) = \mu_j \hat{u}(t; 1) + (1 - \mu_j) \hat{u}(t; 0), \quad j = 1, \dots, N. \quad (20)$$

With  $NM$  new continuous variables  $x_n$  given by

$$x_{(j-1)M+i} = U_i(t_j), \quad i = 1, \dots, M \text{ and } j = 1, \dots, N \quad (21)$$

and  $N$  additional binary variables

$$x_{NM+j} = \mu_j, \quad j = 1, \dots, N \quad (22)$$

the equations (18), (19) and (20) can be written as a mixed integer linear equation system  $Ax = b$  in  $x_1, \dots, x_{(N+1)M}$  with sparse coefficient matrix  $A$ . The integral part of the cost function (4) as used in the examples is approximated by

$$\sum_{i=1}^{NM} (x_i - z_i)^2 = (x - z)^\top (x - z) = x^\top x - 2z^\top x + z^\top z, \quad (23)$$

where  $z_i$  is a discretization of  $u_d$ . Using that  $z^\top z$  is constant, these costs can be written as  $x^\top Qx - c^\top x$  with  $Q = 1$  and  $c = 2z$ . Moreover, the switching costs  $\sum_{\tau_k} \gamma(\tau_k)$  for constant  $\gamma$  can be encoded in  $Q = (q_{i,j})$  by setting  $\kappa = \gamma/N$ ,  $q_{i,i} = \kappa$ ,  $q_{i+1,i} = -\frac{1}{2}\kappa$  and  $q_{i,i+1} = -\frac{1}{2}\kappa$  for  $i = 1 = NM + 1, \dots, (N + 1)M$ . We remark that for stability of the applied methods the above discretization scheme requires  $N$  and  $M$  chosen such that the CFL-condition holds.